Bulletin of the Seismological Society of America, Vol. 88, No. 4, pp. 1003–1013, August 1998

Global CMT Analysis of Moderate Earthquakes, $M_w \geqq 4.5$, Using Intermediate-Period Surface Waves

by Ronald Arvidsson* and Göran Ekström

Abstract A new method for calculating centroid moment tensor (CMT) solutions for moderate-sized earthquakes is presented and tested. In the new algorithm, which is a modification to the standard Harvard CMT method, intermediate-period surface waves are included in the inversion for source parameters. The dispersion of teleseismic surface waves in the period range 40 to 150 sec is predicted by interpolation of recent global phase velocity maps. The method is tested on a set of 20 moderate and large ($5.2 \leqq M_w \leqq 7.2$) earthquakes with known mechanisms. The retrieved mechanisms are similar to the previous results, even when noise is added to the seismograms to simulate earthquakes of a smaller magnitude ($M_w \sim 4.5$). The inversion algorithm is applied to the 1993 Klamath Falls mainshock and aftershock sequence, and the results compare well with earlier results. A catalog of $M_w \geqq 4.5$ focal mechanisms for Greece and surrounding areas for the first six months of 1995 is derived using the new method of analysis.

Introduction

The introduction of digitally recorded seismograms, about two decades ago, together with faster computers and the development of focal mechanism determination techniques (e.g., Dziewonski and Gilbert, 1974; Langston and Helmberger, 1975; Kanamori and Stewart, 1975; Romanowicz, 1982; Kawakatsu, 1995) made routine processing of earthquake source parameters possible on a global scale. Since the early 1980s, Harvard centroid moment tensor (CMT) solutions (Dziewonski *et al.,* 1981; Dziewonski and Woodhouse, 1983) have been routinely obtained for earthquakes of $M_w \geqq 5.0$, and USGS moment tensor solutions (Sipkin, 1982) have been obtained for earthquakes of $M_w \geqq 5.5$. The Harvard CMT method uses body waves filtered with periods greater than 45 sec and, for large events, long-period ($T > 135$ sec) mantle waves, in the inversion for the seismic moment tensor. The USGS routine analysis involves the modeling of the vertical long-period P waves. To date, the Harvard CMT method has resulted in a data base, which, on a global scale, is nearly complete for moment magnitudes of $M_w \geqq 5.5$ for the years 1977 until the present.

Analysis of comprehensive catalogs of focal mechanisms has allowed an improved understanding of the dynamics of, for example, continental collision and overall deformation of the upper mantle as significant as results derived from modern space geodetic methods (e.g., Jackson *et al.,* 1994). There are, however, many tectonically active areas, where earthquakes with $M_w \leqq 5.0$ are common, but with no larger recorded modern event. The smaller events often constitute the only information about the current deformation in that particular region until modern geodetic measurements are collected. In order to analyze these smaller earthquakes, it is possible to make use of regional networks for earthquake focal mechanism determinations. For regions with dense local or regional networks, such as the western United States and Japan, some recently developed methods use, for example, surface waves (Fukushima *et al.,* 1989, Patton and Zandt, 1991; Romanowicz *et al.,* 1993; Ritsema and Lay, 1993; Thio and Kanamori, 1995), body waves (Dreger and Helmberger, 1993; Kawakatsu, 1995), full waveforms (Nábělek and Xia, 1995), and near-field three-component waveforms (Urhammer, 1992) and have been employed on a routine basis. A major limitation is that in many areas around the world, there are no dense seismic networks, thus prohibiting the calculation of earthquake moment tensors. It would constitute an important advance if global networks could be used for source studies of small earthquakes regardless of their locations.

The only signal from small earthquakes that is recorded with high signal-to-noise ratio on the global networks are intermediate-period surface waves. However, it has not been possible to routinely use these waves in source studies because their propagation characteristics are not well predicted by current global three-dimensional (3D) Earth models. However, with recent advances in mapping the dispersion of surface waves, with periods as short as 35 sec, on a global scale (e.g., Trampert and Woodhouse, 1995; Ekström *et al.,*

*Present address: Seismological Department, Uppsala University, Box 2101, S-750 02 Uppsala, Sweden.

1997), we may have advanced sufficiently in our ability to predict surface-wave dispersion to attempt to use them in source studies.

The aim of the current study is to investigate the possibility of extending the Harvard CMT type of analysis to smaller earthquakes on a global scale using intermediate-period surface waves. We first perform a series of experiments to explore the validity of using surface waves with periods as short as 40 sec in global source studies. We then investigate whether smaller earthquakes ($M_w \leqq 4.5$) are recorded with adequate signal-to-noise ratio for this type of analysis. Finally, we systematically apply the new method of CMT analysis to a previously studied sequence of earthquakes in Oregon and to the seismicity of Greece.

Data and Methodology

The method of analysis employed in this study follows closely the standard CMT algorithm (Dziewonski *et al.*, 1981; Dziewonski and Woodhouse, 1983), with some important differences. In the standard CMT analysis, long-period seismograms are matched in two frequency bands: For moderate earthquakes ($M_w \leqq 6.0$), complete body waves arriving before the fundamental-mode surface wave are matched in a passband that has a low-pass cutoff period of 45 sec. For large earthquakes ($M_w > 6.0$), longer-period ($T > 135$ sec) surface waves are also matched in the analysis. The synthetic waveforms used in the analysis are constructed by summation of the Earth's normal modes, and the 3D mantle structure is accounted for using the path average approximation (e.g., Dziewonski *et al.*, 1984).

In the modified CMT analysis presented here, the first arriving surface waves (G1, R1) are filtered with a low-pass cutoff period in the range 40 to 60 sec and then included in the analysis. These waves have previously not been included in the CMT analysis, because they exhibit very significant travel-time delays and advances, owing to their sensitivity to the highly heterogeneous structure of the lithosphere and crust. These variations have not been adequately predicted by earlier models of 3D Earth structure.

We modify the calculation of synthetic seismograms by combining the mode summation for the overtone contribution of the seismogram with a synthesis of the fundamental-mode surface wave by considering it as a traveling wave. This allows us to predict the dispersion of the surface wave using recent global phase velocity maps. Specifically, we calculate the excitation of the fundamental-mode surface wave in the spherical Earth model PREM (Dziewonski and Anderson, 1981) and calculate the propagation dispersion by interpolating the global phase velocity maps derived by Ekström *et al.* (1997) for the period range 35 to 150 sec. These maps are expanded in spherical harmonics up to degree 40 and contain a large amount of detailed heterogeneity not present in global 3D Earth models.

In the calculations presented here, the overtone contributions to the seismograms were corrected using the 3D mantle model S20U7L5 (Ekström and Dziewonski, 1995), and the fundamental modes were corrected using the average phase velocity calculated along the great circle path from a set of preliminary phase velocity maps that are nearly identical to the published maps (Ekström *et al.*, 1997). The applied phase corrections can be as large as one cycle at a period of 60 sec. The attenuation was calculated from the QL6 model (Durek and Ekström, 1996).

The centroid depths in the crust were restricted to be at least 15 km, in order to minimize the instabilities in the moment tensor components $M_{r\theta}$ and $M_{r\varphi}$ at very shallow depths.

The data used in the present study have been collected from the Global Seismograph Network for earthquakes that occurred in 1995 (Table 1). In the first stage in the processing, the instrument responses were removed and the seismograms were resampled and low-pass filtered below 40 sec. All three-component seismograms were rotated into radial and transverse components in order to separate Love and Rayleigh waves. To mix the Love and Rayleigh waves is not recommended because for certain paths the errors in the prediction of the two wave types may be quite different.

The CMT solutions were obtained in repeated inversions. In every inversion, the CMT was derived by an iterative least-squares method that minimizes the difference between the selected and model waveforms (Dziewonski *et al.*, 1981). Seismograms from 70 to 90 stations were screened and edited for each event before every inversion in order to identify bad components with a poor match between synthetic and observed seismograms. These were then not used in the subsequent inversion.

Surface waves are affected more by heterogeneities in the Earth structure than body waves of the same frequency. Hence, fewer components were generally usable for the surface-wave analysis than for body-wave inversions. Stations at distances greater than 90° were usually not included in the surface-wave inversions, except in some cases where the records clearly were of good quality with a good match between synthetics and observed waveforms. We have here focused our analysis on surface waves. Long-period body waves can also be used for the small earthquakes, but due to their smaller amplitudes, they are usually lost in the microseismic noise.

Surface-Wave CMT

Surface-Wave CMT—Large Earthquakes

We first applied the intermediate-period surface-wave CMT methodology to 20 moderate to large shallow earthquakes from 1995, in order to test its performance on events with known source parameters. The earthquakes were selected to represent a variety of geographical locations and have magnitudes in the range $5.2 \leqq M_s \leqq 7.2$ (see Table 1). The inversions were generally stable with small changes from iteration to iteration. After an initial analysis, it was

possible to identify records that were clearly mismatched, primarily due to inadequate Earth models. These seismograms were not used in subsequent inversions. We did not further investigate why certain paths were not well predicted by the dispersion model. Although this editing of the data set improved the overall fit to the data, it did not significantly change the retrieved source parameters.

Figure 1 shows examples of observed and corresponding synthetic waveforms for the 23 February 1995 east of Honshu (M_w = 6.1) earthquake. The waveforms correspond to stations at distances $12° \leqq \Delta \leqq 124°$. Both Love and Rayleigh waves are well matched in spite of clear observed and predicted deviations of surface-wave travel times from the global average at some stations. Figure 2 shows waveforms in the distance range $8° \leqq \Delta \leqq 100°$ for the 21 July 1995 Gansu, China (M_w = 5.7), earthquake. There are travel-time and amplitude discrepancies between observed and predicted waveforms at some stations, for example, the Love wave observed at HRV. However, travel-time differences of less than a quarter of a period and amplitude differences by as much as a factor of 2 at a few stations do not, in general, appear to significantly change the final focal mechanism.

The overall correspondence between the standard CMT mechanisms and those derived using the intermediate-period surface waves is good (Fig. 3). For some events, the differences between the source mechanisms are noticeable, but for no event is there a disagreement over the general geometry or style of faulting. Differences in the centroid locations were usually of the order 10 to 30 km, but larger deviations were also observed, particularly for events in the southern hemisphere. The differences between the regular Harvard centroid origin time and the one derived from the surface waves are generally small. Most likely, the differences in the centroid location and time can be ascribed to the different station coverage for the standard CMT analysis and the new analysis, and remaining shortcomings in the Earth model applied, in particular in the prediction of the surface-wave phase.

Surface-Wave CMT—Simulation of Small Earthquakes

As a second test, we used the same set of 20 earthquakes but added ground noise in order to simulate the signal-to-noise ratio for a smaller earthquake. Specifically, we extracted ground noise from each individual station and added these records to scaled earthquake seismograms, for which the signal amplitude had been reduced to correspond to an earthquake of M_s = 4.5.

From the surface-wave magnitude formula that is written as $M_s = \log A + 1.66 \log\Delta + C$, where A is amplitude, Δ is distance, and C is a constant, we find a scaling relation

$$A_{4.5} = 10^{4.5}/10^{M_s},$$

where $A_{4.5}$ is the factor used to scale the observed seismograms of an earthquake with magnitude M_s to correspond to an earthquake of M_s = 4.5.

The inversion results for the simulated small earthquakes (Fig. 3) show a good resemblance both to the standard Harvard CMTs as well as to the surface-wave CMTs derived in the previous section. We find that the differences between the surface-wave CMTs and the standard Harvard CMTs are larger than between surface-wave CMT solutions

Table 1
Earthquakes Used in Test of Surface-Wave CMT

Ev	Year	Mo	D	H	Mi	Sec	Lat	Lon	H	M_s	Area
1	1995	1	19	15	5	4.0	4.90	−73.10	33.0	6.5	Colombia
2	1995	2	23	5	1	25.0	39.60	143.80	33.0	5.9	Off east coast of Honshu
3	1995	4	14	0	32	55.0	30.30	−103.30	10.0	5.6	Western Texas
4	1995	4	17	23	28	8.0	45.90	151.30	33.0	6.3	Kuril Islands
5	1995	4	23	2	55	56.0	51.30	179.50	33.0	6.4	Rat Islands, Aleutian Islands
6	1995	5	4	0	34	12.0	40.67	23.47	28.0	5.1	Greece
7	1995	5	8	18	8	10.0	11.60	126.10	33.0	6.2	Philippine Islands region
8	1995	5	13	8	47	15.0	40.00	21.60	33.0	6.6	Greece
9	1995	5	31	16	8	38.0	18.80	−107.50	33.0	6.0	Off coast of Jalisco, Mexico
10	1995	6	14	11	11	47.0	12.00	−88.30	33.0	6.0	Off coast of Central America
11	1995	6	15	0	15	51.0	38.40	22.20	33.0	6.5	Greece
12	1995	6	30	11	58	54.0	24.40	−110.30	10.0	6.1	Baja California, Mexico
13	1995	7	21	22	44	8.0	36.40	103.30	33.0	5.6	Gansu, China
14	1995	4	29	9	44	0.0	11.70	125.90	33.0	6.0	Samar, Philippine Island
15	1995	7	11	21	46	42.0	22.00	99.30	33.0	7.2	Myanmar China border reg.
16	1995	7	12	15	46	58.0	−23.30	170.50	33.0	6.4	Loyalty Islands region
17	1995	8	28	10	46	10.0	25.90	−110.30	10.0	6.3	Gulf of California
18	1995	9	14	14	4	33.0	16.77	−98.60	25.0	7.2	Mexico
19	1995	9	22	5	39	29.0	−6.00	146.54	33.0	6.0	East Papua New Guinea region
20	1995	11	24	6	18	57.1	−42.99	171.62	10.0	6.4	South Island, New Zealand

Ev, event; Mo, month; D, day of month; H, hour; Mi, minute; Sec, seconds; Lat, latitude; Lon, longitude; H, focal depth; M_s, surface-wave magnitude.

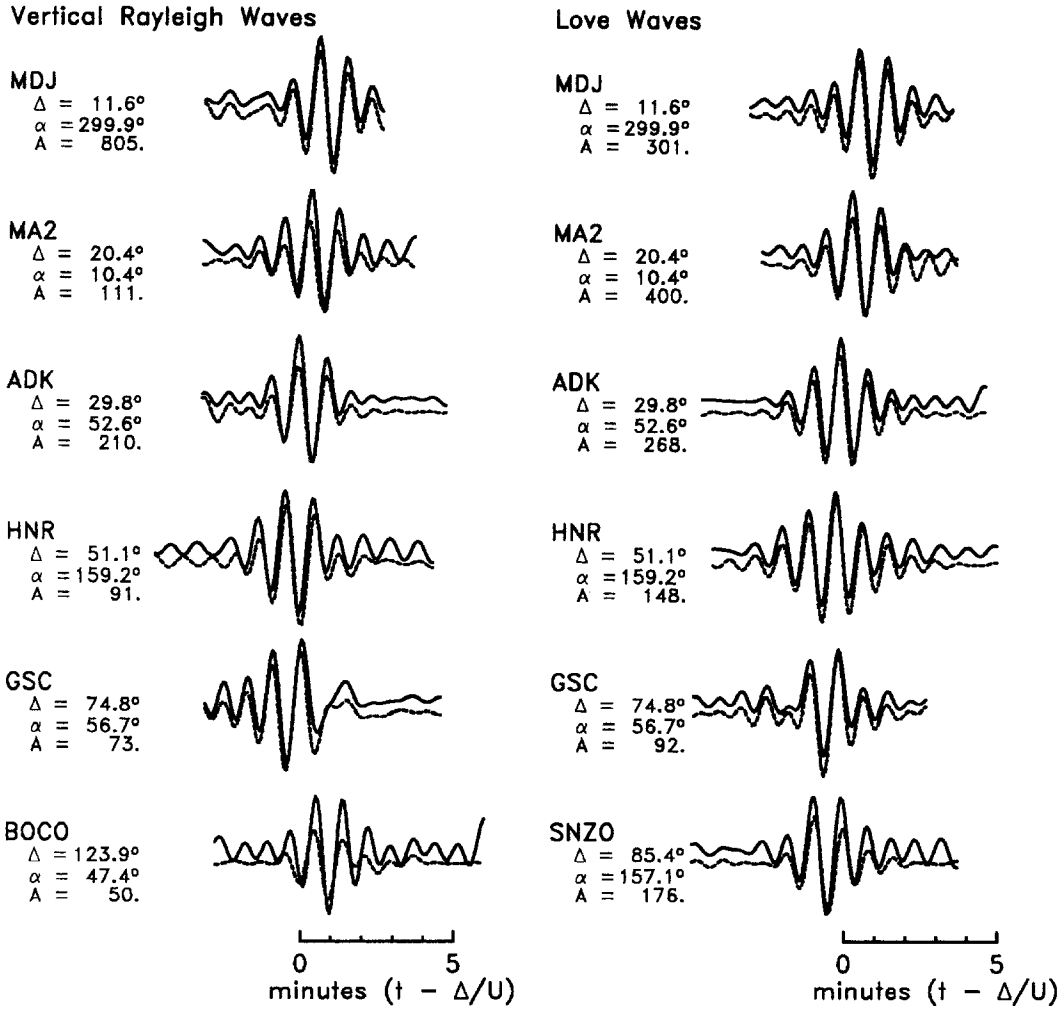

Figure 1. Observed (solid lines) and synthetic seismograms (broken lines) for event 2 (Table 1), the M_w = 6.1, 23 February 1995, East of Honshu earthquake. Left column, Rayleigh waves; right column, Love waves. Δ, epicentral distance; α, azimuth; A, relative amplitude; U, group velocity.

with and without noise (Fig. 3). This suggests that, for this set of earthquakes, the Earth model has a larger impact on the CMT mechanism than the amplified noise in the seismograms for the simulated small earthquakes.

A further indication of the consistency of the recovery of the source mechanism can be obtained by examining the non-double couple (NDC) component of the moment tensors. We observe that out of 20 events, 16 show the same sign of the NDC for the surface-wave CMT for the large and simulated small earthquakes, indicating that the noise is important for the NDC component in only a few cases. Examination of solutions from earthquakes from northern South America to Mexico shows that most of them have a strong similarity between the surface-wave and the standard CMT. The impact of noise on the simulated small-earthquake CMT solutions is shown by larger deviations between this set of solutions and the regular CMT than when compared with the surface-wave CMT.

The scalar moments obtained in the standard CMT and the surface-wave CMT agree well (Fig. 4). The surface-wave CMTs had, on average, 5% smaller moments than the standard solutions. For the simulated small events, the scalar moments are on average 24% larger. Some events show larger differences, up to a factor of 2. These discrepancies are most likely an effect of differences in the focal mechanisms, because the smallest differences are observed when the retrieved focal mechanisms are very similar. Additional experiments show that differences in the source depth cannot explain the moment differences, as also discussed in the next section.

The 1993 Klamath Falls, Oregon, Earthquake Sequence

Moment tensor inversions of the 1993 Klamath Falls, Oregon, earthquake sequence have been presented by Braunmiller *et al.* (1995) and Dreger *et al.* (1995). Full waveform inversion was the main analysis tool used by both groups.

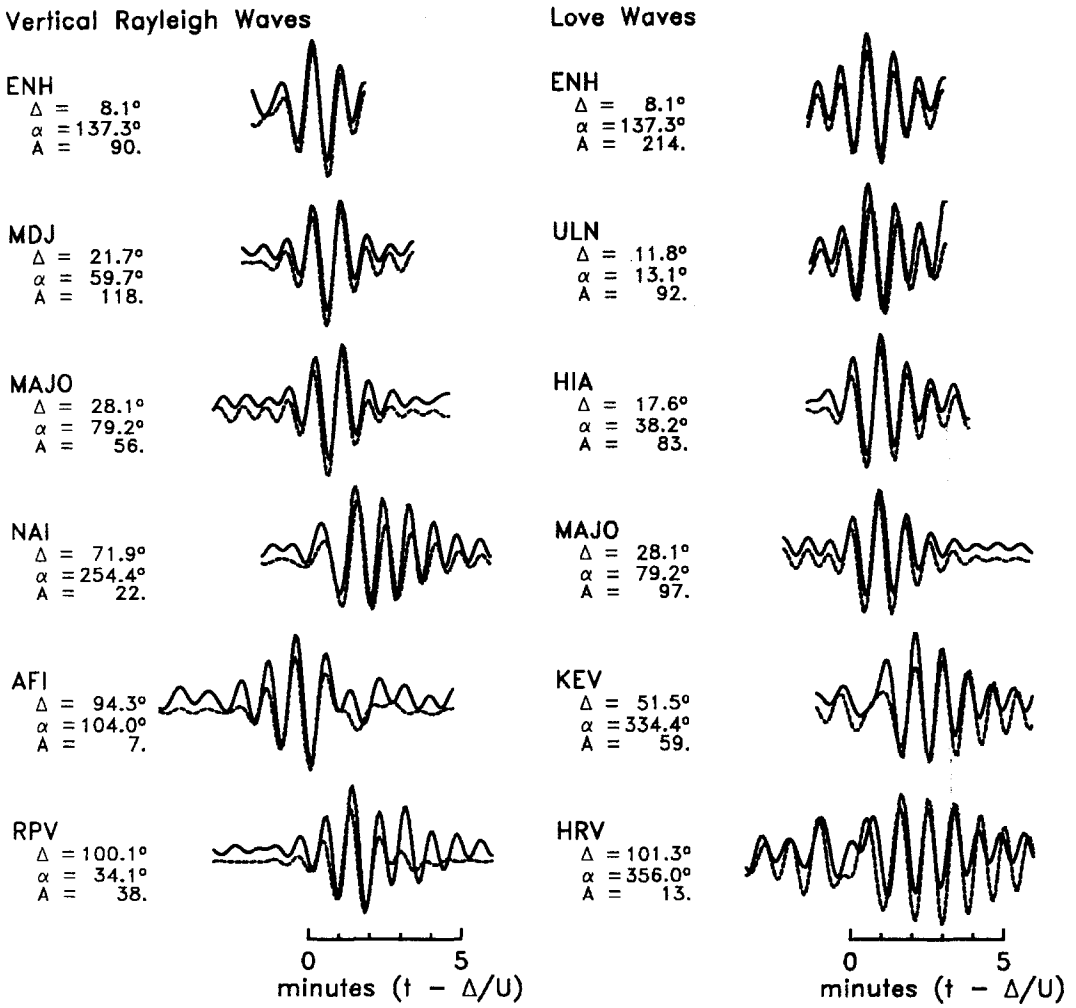

Figure 2. Observed (solid lines) and synthetic seismograms (broken lines) for event 13 (Table 1), the M_w = 5.7, 21 July 1995, Gansu, China, earthquake. Left column, Rayleigh waves; right column, Love waves. Δ, epicentral distance; α, azimuth; A, relative amplitude; U, group velocity.

Dreger *et al.* (1995) derived single-station three-component solutions for the smaller events ($M_w < 5.0$), while Braunmiller *et al.* (1995) employed a larger number of seismograms in their analyses. The two studies resulted in moment tensors for 20 earthquakes with $3.8 \leqq M_w \leqq 6.0$ using data from the local western U.S. networks and nearby IRIS GSN stations.

We applied the intermediate-period surface-wave CMT method to the earthquakes in the sequence with $m_b \geqq 4.0$ or $M_s \geqq 4.0$ and data from the GSN. We were able to derive CMT mechanisms for 10 earthquakes, with the smallest M_w = 4.4. Table 2 gives a comparison of our results with those of Braunmiller *et al.* (1995) and Dreger *et al.* (1995). The largest deviations between our results and those of the other groups are for the smallest events. Rather large differences in moments are also observed for the smallest earthquakes, up to a factor larger than 3, whereas for the larger events, it is less than 2. Our moments were in all cases larger. It is not clear what the explanation is for this disagreement. The deeper centroid depth for our mechanisms may partly explain moment differences because shallow crustal events excite stronger surface waves than events deeper in the crust. To test what impact the depth had upon our moments, we computed synthetics for depths ranging from 5 to 25 km. The differences were less than a factor of 2 for the Rayleigh waves and much smaller for the Love waves. Thus, depth alone cannot explain the moment differences. Even though we observe a relatively small difference between the surface-wave CMT and the regular Harvard CMT, it is difficult from this single comparison with the methods used from the other studies to deduce which method fails in the moment determination. It should be observed that the largest differences in moment are between the smallest events. It can be that biases from all methods and differences of the mechanisms between the methods account for the moment differences observed in Table 2. The applied attenuation model cannot be responsible for the differences in moment. The paths we used are short, and the effect of attenuation is small.

Figure 3. Centroid moment tensor solutions for events 1 to 20 (Table 1), for each triplet of solutions. Left column, regular Harvard CMT; center column, surface-wave CMT; right column, surface-wave CMT with noise added to simulate smaller earthquakes.

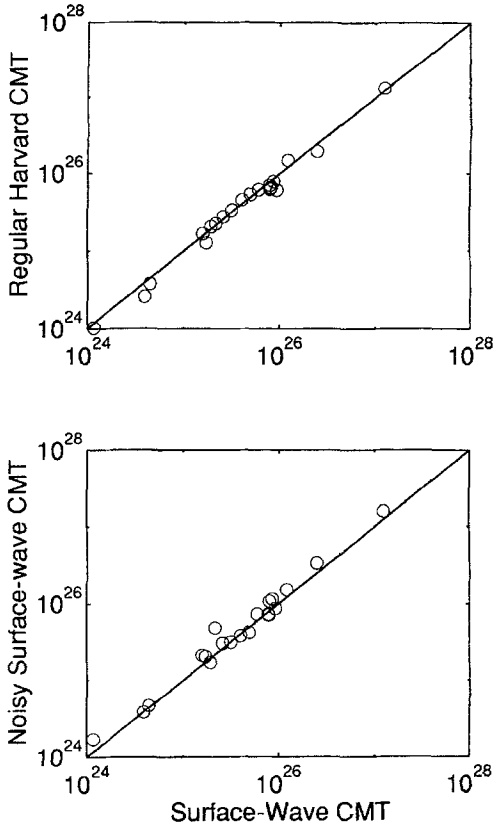

Figure 4. (a) Regular CMT moments versus surface-wave CMT moments. (b) Regular CMT moments versus simulated small-earthquake surface-wave CMT moment.

As expected, there is a considerable amount of noise in the seismograms of the smallest earthquake (M_w = 4.4) that we were able to analyze, but, nonetheless, the inversion result is stable, and the synthetics fit the observed data well (Fig. 5). The focal geometry agrees well with the previous studies (Table 2), but our derived moment is more than three times larger than the one derived by Dreger *et al.* (1995). The earthquake mechanisms (Fig. 6) fit into three groups (Braunmiller *et al.*, 1995) with the first group dominated by the first mainshock believed to have propagated along the Lake of the Woods fault segment B. The second mainshock occurred on segment C and the largest aftershock on segment A. Our aftershock mechanisms follow this pattern of faulting with the northernmost mechanisms showing a change in strike from northwest–southeast to nearly north–south.

A Regional CMT Catalog for Greece, January to June, 1995

In our final experiment, a moment tensor bulletin for Greece was produced for the first half of 1995. One incentive for testing the surface-wave CMT on smaller earthquakes in the area of Greece is that it is a key area for tectonic studies. Greece is, to cite Jackson (1995), "a special case—a natural laboratory for continental tectonics." The main deformation is accommodated by strike-slip movements in the east where the Anatolian block is moving westward due to the northward movement of Arabia and its collision with Eurasia in the north (McKenzie, 1972). In the west, the Aegean block is extending in a north–south direction due to clockwise rotations of rigid crustal blocks (e.g., Taymaz *et al.*, 1991; Jackson *et al.*, 1992; Le Pichon *et al.*, 1995) that are caused by the westward drift of Turkey and sinking of the slab in the Hellenic trench. Along the Hellenic trench, thrust faults are common due to subduction. How the blocks are formed that are rotating in the mainland of Greece and Peloponessos is not clear. A larger number of focal mechanisms than what is presently available would clearly add more information relevant to these issues.

The area from which we selected earthquakes for analysis extends from 34° to 42° in latitude and 18° to 27° in longitude. All events with a reported m_b or $M_s \geqq 4.5$ were analyzed. It is probable that some events may have had underestimated magnitudes and are thus lost from the present analysis. The 49 earthquakes selected for analysis occurred in such different areas as the subduction zone in the Hellenic arc south of Crete, the Ionian sea, and mainland Greece, thus sampling different tectonic environments.

A total of 33 surface-wave CMT solutions were derived (Table 3) with the smallest earthquake having a magnitude M_w = 4.1. For some of the small events, we found it nec-

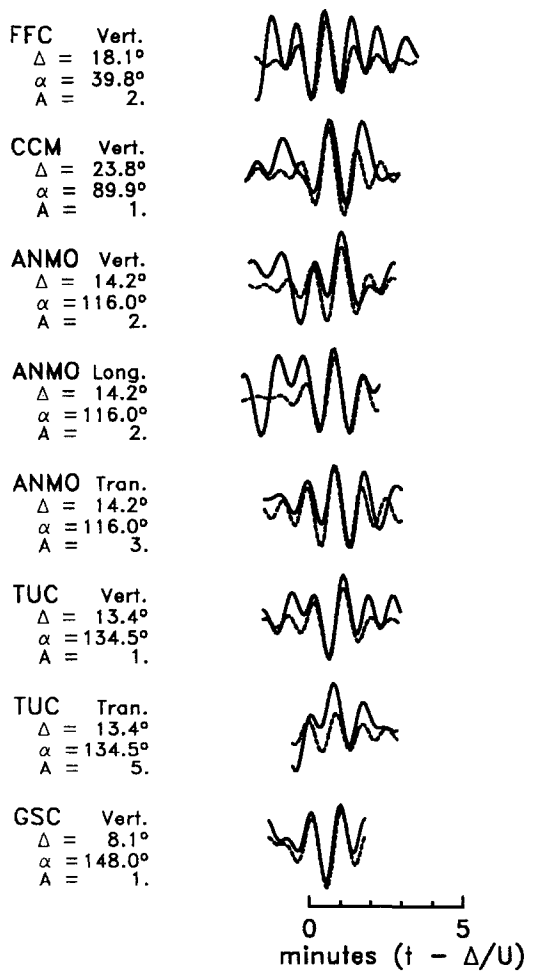

Figure 5. Observed (solid lines) and synthetic seismograms (broken lines) for the 21 September 1993, 03:16, Klamath Falls, Oregon, M_w = 4.4, earthquake. Vert., vertical Rayleigh waves; Long., longitudinal Rayleigh waves; Tran., transverse Love waves; Δ, epicentral distance; α, azimuth; *A*, relative amplitude; *U*, group velocity.

essary to hold the centroid location fixed at the reported hypocenter. This is primarily a consequence of limited station coverage. Examples of observed and corresponding synthetic seismograms for the 14 May M_w = 4.6 aftershock of the 13 May northern Greece earthquake are shown in Figure 7. Though for earthquakes of this size the majority of useful seismograms are obtained at distances less than 40°, an occasional useable surface wave is sometimes observed at distances greater than 70°, such as at FFC for this event.

There are several reasons why we were not able to determine surface-wave CMT solutions for all 49 earthquakes initially selected for analysis. Magnitude estimates for smaller earthquakes are generally less reliable than for larger earthquakes. In addition, seismic ground noise is not stationary, and when small earthquakes occur as aftershocks, the signal of the mainshock often precludes a detailed analysis of the smaller event.

Table 2
Earthquake Source Parameters—Klamath Falls, Oregon, Earthquake Sequence

Study	OT	Lat.	Lon.	M_w	M_0	Depth	Strike	Dip	Rake
1	9309210316	42.31	122.02	4.4	5.3e15	19	321	63	−110
2				4.2	2.6e15	6	331	45	−114
3				4.1	1.8e15	8	326	57	−103
1	9309210329	42.32	122.03	6.0	1.3e18	15	335	58	−93
2				6.0	1.1e18	9	331	47	−105
3				5.9	7.6e17	8	332	55	−94
3.2				5.9	8.4e17	12	353	37	−59
3.3				6.0	1.1e18	8	343	46	−83
4				6.0	1.1e18	15	334	60	−98
1	9309210416	42.27	122.01	4.7	1.0e16	15	352	34	−58
2				4.5	7.1e15	6	339	23	−97
3				4.5	7.2e15	8	358	34	−41
1	9309210434	42.30	122.04	4.6	7.2e15	15	277	76	−109
2				4.3	3.6e15	6	320	50	−117
3				4.3	2.8e15	5	308	53	−129
1	9309210545	42.36	122.06	6.0	1.2e18	15	343	53	−98
2				6.0	1.1e18	9	351	42	−91
3				5.9	7.9e17	8	346	46	−89
3.2				6.0	1.4e18	12	9	37	−46
3.3				6.0	1.1e18	8	352	4	−84
4				6.0	1.0e18	15	357	34	−85
1	9309210614	42.39	122.05	4.9	2.9e16	17	8	54	−92
2				4.9	2.1e16	5	355	52	−101
3				4.8	2.0e16	8	3	56	−90
1	9309230621	42.31	122.05	4.7	1.3e16	15	344	51	−90
2				4.5	7.4e15	3	353	46	−94
3				4.6	8.7e15	8	328	45	−117
1	9309241653	42.38	121.97	4.5	9.0e15	29	180	45	−90
2				4.0	1.2e15	3	330	38	−104
3				4.0	1.3e15	5	182	63	−22
1	9312042215	42.29	122.01	5.5	2.4e17	15	330	57	−91
2				5.5	2.0e17	6	331	48	−96
3				5.4	1.4e17	8	335	50	−83
3.2				5.4	1.5e17	10	330	42	−72
3.3				5.4	1.6e17	6	326	45	−79
1	9401192227	42.29	121.94	4.6	5.2e15	18	315	66	−102
2				4.1	1.7e15	6	346	34	−91
3				4.2	2.1e15	5	353	42	−70

Lat., latitude; Lon., longitude; M_0, seismic moment; 1, this study; 2, full waveform inversion (Braunmiller *et al.*, 1995); 3, body-wave inversion (Dreger *et al.*, 1995); 3.2, spectral surface-wave inversion (Dreger *et al.*, 1995); 3.3, RCMT (Dreger *et al.*, 1995); 4, Harvard CMT (Dziewonski *et al.*, 1994). Locations from Dreger *et al.* (1995).

The surface-wave CMT solutions for the first six months of 1995 reflect several of the ongoing tectonic processes discussed earlier (Fig. 8). One mechanism south of Crete shows thrust faulting of a geometry that can be expected as a consequence of subduction, but other faulting geometries are also seen. Earlier solutions with similar mechanisms are found in the Harvard CMT catalog. In the northwest, one event has thrust faulting that is consistent with the collision between the Adriatic–Apulia platform and Greece–Albania. In the mainland of Greece, all events, as expected, show normal faulting styles reflecting the extension of the crust.

It is obvious that mechanisms from this short time span will not resolve any major tectonic issues, but this study

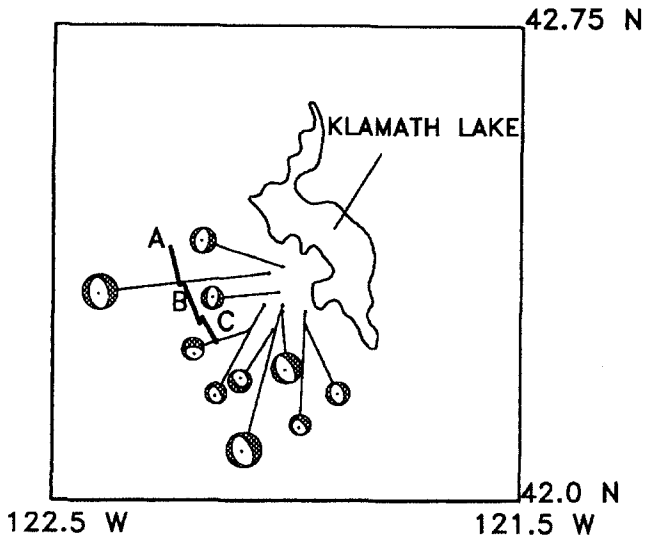

Figure 6. Surface-wave CMT solutions for the 1993 Klamath Falls earthquake sequence. A, B, and C denote three main segments of the Lake of the Woods fault zone. The smallest CMT mechanism corresponds to an $M_w = 4.4$ earthquake and the largest mechanism to an $M_w = 6.0$ event.

shows that a much shorter time span is needed in order to get information on the overall deformation by lowering the magnitude threshold level for deriving stable CMT solutions. For comparison, in the Harvard CMT catalog, there are 113 CMT solutions within the investigated region, corresponding to a time period of 20 years, whereas we were able to derive 33 additional CMT solutions for a six-month period.

Discussion and Conclusion

Our experiments suggest that the approach of inverting intermediate-period Rayleigh and Love waves, recorded primarily at teleseismic distances, for the determination of earthquake source parameters for relatively small earthquakes is feasible on a global scale. A necessary condition for the success is the ability to predict surface-wave travel times with sufficient accuracy. Our implementation of recent global phase velocity maps (Ekström *et al.*, 1997) for this purpose appears to satisfy this condition, as demonstrated by our experiments.

The adjustment of phase velocities for inversion of the moment tensor by means of surface waves is not new (e.g., Romanowicz, 1982; Patton and Zandt, 1991) but has previously not been applied to the global problem because the earlier Earth models were not of sufficient accuracy. Based on our experiments, it would seem feasible to extend the current threshold of approximately $M_w \sim 5.0$ for the standard CMT analysis to at least $M_w \sim 4.5$ or approximately a factor of 7 in moment. As demonstrated, certain regions, like the continental United States and Greece, may have even lower magnitude threshold. This would give an increased data base for a given region of at least three times if the level

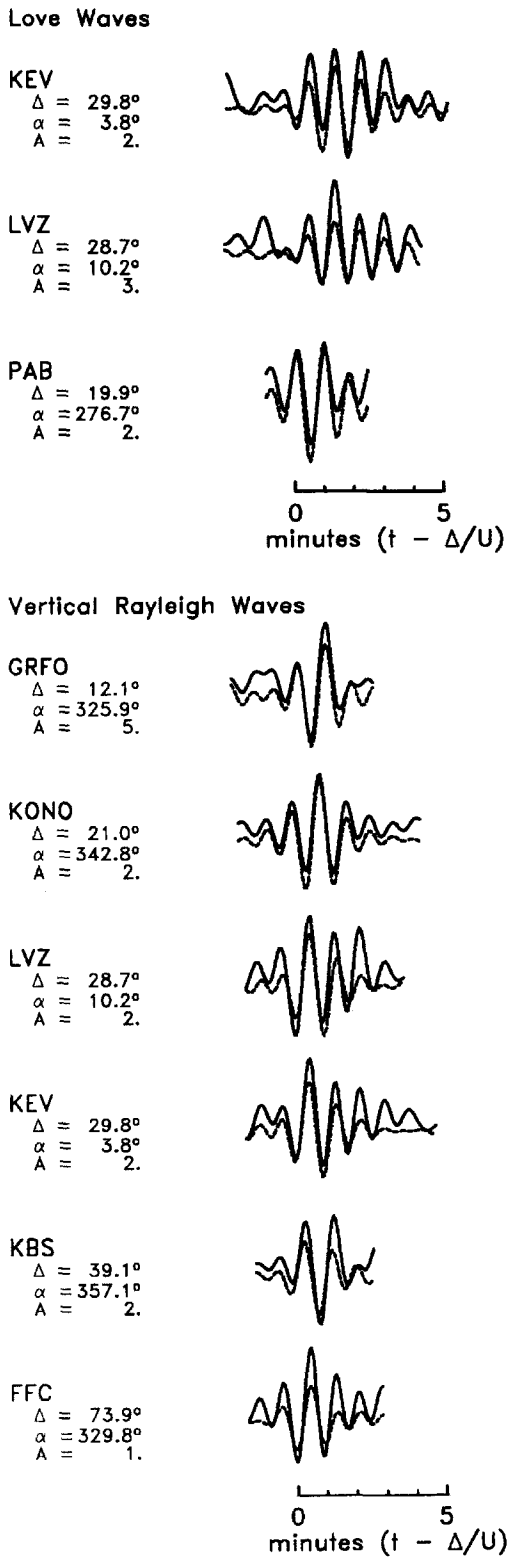

Figure 7. Observed (solid lines) and synthetic seismograms (broken lines) for the 14 May, northern Greece, $M_w = 4.6$, earthquake. Δ epicentral distance; α, azimuth; A, relative amplitude; U, group velocity.

of completeness follows similar trends between the regular CMT and the methodology presented in this article and if the global cumulative Gutenberg–Richter b-value is close to 1.

Table 3
Surface-Wave CMT Solutions, Greece, January–June, 1995

Year	M	D	H	Mn	S	M_0	CT	Lat.	Lon.	h	M_w	s	d	r	s	d	r	m_1	m_2	m_3	m_4	m_5	m_6
1995	1	3	22	51	44.8	2.99e23	0.2	34.90	23.62	15	4.9	359	17	176	94	89	74	0.04	−0.01	−0.03	0.96	−0.07	0.29
1995	1	7	20	30	47.7	3.25e23	3.7	37.95	19.83	19	4.9	134	36	−78	300	55	−98	−0.79	0.61	0.18	0.30	−0.13	−0.66
1995	2	3	22	29	9.6	2.28e23	3.5	34.22	25.19	15	4.8	183	7	−76	350	83	−92	−0.01	−0.42	0.43	0.16	−0.96	−0.12
1995	2	16	13	2	18.2	3.41e23	4.6	34.32	26.56	15	5.0	230	26	−22	340	80	−115	−0.30	−0.25	0.54	0.34	−0.78	0.22
1995	3	30	18	17	15.6	1.73e23	−1.5	34.37	24.56	22	4.8	82	46	121	221	51	62	0.80	−0.75	−0.05	0.03	−0.26	−0.61
1995	5	3	21	36	52.3	1.14e23	−1.9	40.26	23.90	16	4.6	56	45	−123	279	54	−62	−0.80	0.98	−0.18	0.21	−0.29	0.26
1995	5	3	21	43	25.5	1.18e23	−0.5	40.32	23.83	16	4.7	259	45	−90	79	45	−90	−0.92	1.03	−0.12	−0.04	−0.03	0.24
1995	5	4	0	34	12.0	1.15e24	−3.3	40.31	23.78	19	5.3	280	40	−74	79	52	−103	−0.93	0.99	−0.06	−0.20	−0.17	0.01
1995	5	8	5	11	9.9	8.71e22	−1.7	38.27	22.36	17	4.6	84	45	−113	294	50	−69	−0.95	0.94	0.00	−0.04	−0.29	−0.17
1995	5	9	1	14	37.0	2.42e23	1.9	40.61	20.87	21	4.9	231	34	−90	51	56	−90	−0.78	0.52	0.25	−0.29	−0.24	0.68
1995	5	13	8	47	12.6	8.28e25	4.0	39.93	21.66	20	6.5	259	40	−79	65	51	−99	−0.94	0.91	0.02	−0.15	−0.16	0.32
1995	5	13	10	58	34.0	3.77e23	0.0	40.06	21.55	15	5.0	205	52	−130	79	53	−51	−0.79	0.47	0.32	−0.51	0.63	0.32
1995	5	13	11	43	28.9	0.89e24	4.3	40.14	21.89	28	5.2	254	44	−84	65	47	−96	−1.20	0.75	0.45	−0.02	−0.13	0.13
1995	5	13	18	5	58.0	1.03e23	9.3	40.28	21.52	29	4.6	46	44	−142	287	65	−52	−0.60	1.11	−0.51	0.38	−0.08	0.30
1995	5	13	19	0	47.9	1.24e23	10.7	40.44	21.61	30	4.7	74	36	−94	258	54	−87	−0.80	1.02	−0.22	0.31	0.09	0.31
1995	5	13	23	56	25.9	1.88e23	−0.6	39.86	21.86	18	4.8	287	48	−41	47	61	−130	−0.62	0.89	−0.26	−0.05	−0.56	0.27
1995	5	14	2	46	58.7	2.72e23	−0.2	39.86	21.62	19	4.9	266	42	−72	63	50	−106	−0.98	0.88	0.10	−0.07	−0.25	0.26
1995	5	14	3	9	35.7	9.09e22	0.3	39.89	21.78	20	4.6	261	46	−75	59	46	−105	−1.04	0.82	0.22	0.06	−0.22	0.25
1995	5	14	5	59	15.8	1.10e23	−1.8	39.80	21.29	15	4.6	308	66	−10	42	81	−156	−0.38	1.10	−0.72	−0.26	−0.20	0.19
1995	5	14	8	35	11.6	4.79e22	7.5	40.33	21.51	19	4.4	300	55	−44	60	55	−136	−0.65	0.70	−0.05	−0.18	−0.90	0.09
1995	5	15	4	13	55.1	8.11e23	0.6	39.82	21.73	20	5.2	257	41	−76	59	50	−102	−0.97	0.84	0.13	−0.08	−0.20	0.35
1995	5	15	8	16	58.7	5.77e22	1.6	40.11	21.45	21	4.4	26	42	−141	265	65	−55	−0.65	0.54	0.11	0.54	−0.18	0.56
1995	5	15	9	1	51.3	5.86e22	3.4	40.16	21.92	15	4.4	30	22	−128	250	72	−76	−0.47	0.39	0.08	0.74	0.29	0.46
1995	5	15	9	19	42.2	5.08e22	2.3	40.09	21.51	31	4.4	298	53	−49	62	53	−131	−0.73	0.95	−0.23	0.02	−0.51	0.08
1995	5	16	4	37	30.6	1.68e23	3.1	40.18	21.30	29	4.8	115	47	−47	241	58	−126	−0.75	0.90	−0.15	0.14	0.55	0.03
1995	5	18	3	48	58.6	9.21e23	−8.5	40.09	21.82	15	5.2	101	45	−75	259	47	−105	−0.95	1.02	−0.07	0.02	0.18	0.00
1995	5	19	6	48	49.3	7.52e23	3.0	39.91	21.53	17	5.2	239	37	−94	64	53	−87	−0.96	0.75	0.21	−0.25	−0.08	0.41
1995	5	20	20	9	30.3	7.34e22	3.8	40.01	21.58	36	4.5	270	45	−90	90	45	−90	−0.90	1.10	−0.20	−0.07	−0.06	−0.08
1995	5	21	4	4	22.9	3.74e22	−5.7	39.70	21.60	15	4.3	300	55	−44	60	55	−136	−0.65	0.86	−0.20	−0.18	−0.68	0.10
1995	5	23	4	37	38.4	4.17e22	4.4	40.09	21.68	23	4.4	284	47	−70	76	47	−110	−1.02	0.89	0.13	0.08	−0.33	0.12
1995	5	24	6	24	6.7	6.36e22	−0.1	40.09	21.68	22	4.5	69	35	−120	284	60	−71	−0.88	0.83	0.05	0.41	−0.35	0.02
1995	5	28	19	56	39.9	1.53e23	−3.6	38.08	21.93	15	4.7	300	41	−57	78	57	−116	−0.81	0.92	−0.10	−0.34	−0.31	−0.19
1995	6	5	5	20	19.8	4.06e22	2.8	39.45	20.26	15	4.3	137	30	90	317	60	90	0.85	−0.39	−0.46	−0.28	0.42	0.45
1995	6	11	18	51	46.7	1.79e23	−0.3	39.72	21.56	19	4.8	260	40	−84	72	51	−95	−1.03	0.87	0.16	−0.19	−0.13	0.19
1995	6	15	0	15	48.6	6.21e25	1.4	38.08	22.21	15	6.5	297	40	−62	82	55	−111	−0.90	0.90	0.00	−0.30	−0.28	−0.16
1995	6	15	4	51	18.4	0.95e23	2.7	38.31	22.34	20	4.6	286	35	−68	80	58	−104	−1.06	0.69	0.37	−0.39	−0.34	−0.07
1995	6	15	7	0	59.3	8.07e22	3.0	38.38	22.37	24	4.5	276	40	−82	85	50	−97	−1.20	0.75	0.45	−0.18	−0.15	−0.05
1995	6	19	15	0	16.6	2.06e22	1.2	39.68	21.68	21	4.1	270	45	−90	90	45	−90	−0.93	1.07	−0.14	0.01	0.35	−0.26

M, month; D, day; H, hour; Mn, minute; S, seconds; M_0, moment; CT, centroid time; Lat., latitude; Lon., longitude; h, centroid depth; M_w, moment magnitude; s, strike; d, dip; r, rake; m_1–m_6, moment tensor components.

The level of completeness for the standard Harvard CMT is approximately $M_w = 5.5$. It is hard to predict what the level would be after systematic application to global seismicity of the surface-wave CMT methodology presented here. It is likely that the level of completeness will vary from region to region. In some areas, it will be close to the results from the Klamath Falls where we found that all earthquakes with $M_w \geqq 4.4$ could be studied. In regions with low density of seismographs, such as the oceans and the southern hemisphere, this threshold will be higher.

We show here that for earthquakes having M_w between 5.2 and 4.5, a dense local digital network is not necessary for determining focal mechanisms. In fact, the surface-wave CMT methodology allows using only global digital stations as demonstrated by the CMT solutions of the Greek earthquakes from the first half of 1995 including the aftershock sequences of the 13 May 1995, $M_w = 6.5$, northern Greece, and the 15 June 1995, $M_w = 6.5$, Gulf of Corinth, earthquakes. The aftershocks, in both cases, have basically the same mechanisms as the mainshocks. In the case of the northern Greece earthquake, observations of fault surface breaks show mainly normal faulting (Pavlides *et al.*, 1995) of the same style as we observe in our CMT solutions of aftershocks (Fig. 8, Table 3).

Acknowledgments

This work has been supported by the Swedish Foundation for International Cooperation in Research and Higher Education under Swedish Natural Science Foundation Contract Dnr 720 22/95. Additional support was provided by NSF Grant EAR-92-19361.

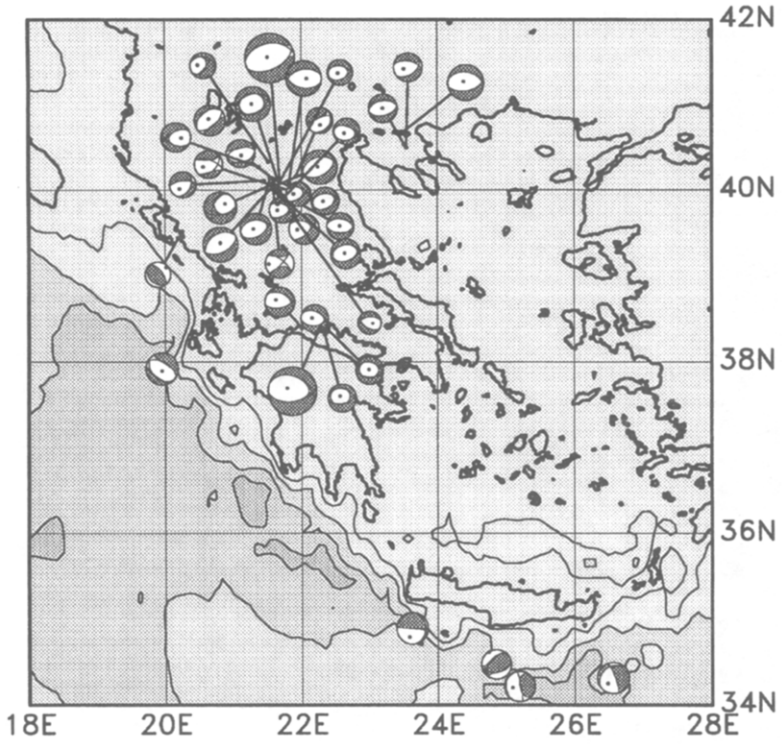

Figure 8. Surface-wave CMT solutions for Greece, January to June, 1995. Included in the map are the four regular CMT solutions produced by Dziewonski *et al.* (1996) during the same time period. The smallest CMT mechanism corresponds to an M_w = 4.1 earthquake and the largest mechanism to an M_w = 6.5 event.

References

Braunmiller, J., J. Nábělek, B. Leitner, and A. Qamar (1995). The 1993 Klamath Falls, Oregon earthquake sequence: source mechanism from regional data, *Geophys. Res. Lett.* **22,** 105–108.

Dreger, D. S. and D. V. Helmberger (1993). Determination of source parameters at regional distances with three-component sparse network data, *J. Geophys. Res.* **98,** 8107–8125.

Dreger, D., J. Ritsema, and M. Pasyanos (1995). Broadband analysis of the 21 September, 1993, Klamath Falls earthquake sequence, *Geophys. Res. Lett.* **22,** 997–1000.

Durek, J. J. and G. Ekström (1996). A radial model of anelasticity consistent with long-period surface wave attenuation, *Bull. Seism. Soc. Am.* **86,** 144–158.

Dziewonski, A. M. and F. Gilbert (1974). Temporal variation of the seismic moment and the evidence of precursive compression for two deep earthquakes. *Nature* **247,** 185–188.

Dziewonski, A. M. and D. L. Anderson (1981). Preliminary reference Earth model, *Phys. Earth Planet. Interiors* **25,** 297–356.

Dziewonski, A. M. and J. H. Woodhouse (1983). An experiment in the systematic study of global seismicity; Centroid moment tensor solutions for 201 moderate and large earthquakes of 1981, *J. Geophys. Res.* **88,** 3247–3271.

Dziewonski, A. M., J. E. Franzen, and J. H. Woodhouse (1984). Centroid-moment tensor solutions for January–March 1984, *Phys. Earth Planet. Interiors* **34,** 209–219.

Dziewonski, A. M., T.-A. Chou, and J. H. Woodhouse (1981). Determination of earthquake source parameters from waveform data for studies of global and regional seismicity, *J. Geophys. Res.* **86,** 2825–2852.

Dziewonski, A. M., G. Ekström, and M. P. Salganik (1994). Centroid-moment tensor solutions for July–September 1993, *Phys. Earth Planet. Interiors* **83,** 165–174.

Dziewonski, A. M., G. Ekström, and M. P. Salganik (1996). Centroid-moment tensor solutions for January–March 1995, *Phys. Earth Planet. Interiors* **93,** 147–157.

Ekström, G. and A. M. Dziewonski (1995). Improved models of upper mantle S velocity structure, *EOS* **76,** F421.

Ekström, G., J. Tromp, and E. W. Larson (1997). Measurements and global models of surface wave propagation, *J. Geophys. Res.* **102,** 8137–8157.

Fukushima, T., D. Suetsugu, I. Nakanishi, and I. Yamada (1989). Moment tensor inversion for near earthquakes using long-period digital seismograms, *J. Phys. Earth* **37,** 1–29.

Jackson, J. (1995). Active tectonics of the Aegean region, *Ann. Rev. Earth Planet. Sci.* **22,** 239–271.

Jackson, J., J. Haines, and W. Holt (1992). The horizontal velocity field in the deforming Aegean Sea region determined from the moment tensors of earthquakes, *J. Geophys. Res.* **97,** 17657–17684.

Jackson, J., J. Haines, and W. Holt (1994). A comparison of satellite laser ranging and seismicity data in the Aegean region, *Geophys. Res. Lett.* **21,** 2849–2852.

Kanamori, H. and G. S. Stewart (1975). Mode of strain release along the Gibbs fracture zone, Mid-Atlantic Ridge, *Phys. Earth Planet. Interiors* **11,** 312–332.

Kawakatsu, H. (1995). Automated near-real time CMT inversion, *Geophys. Res. Lett.* **22,** 2569–2572.

Langston, C. A. and D. V. Helmberger (1975). A procedure for modeling shallow dislocation sources, *Geophys. J. Astr. Soc.* **42,** 117–130.

Le Pichon, X., N. Chamot-Rooke, S. Lallemant, R. Noomen, and G. Veis (1995). Geodetic determination of the Kinematics of central Greece with respect to Europe: implications for eastern Mediterranean tectonics, *J. Geophys. Res.* **100,** 12675–12690.

McKenzie, D. (1972). Active tectonics of the Mediterranean region, *Geophys. J. R. Astr. Soc.* **30,** 109–185.

Nábělek, J. and G. Xia (1995). Moment tensor analysis using regional data: application to the 25 March, 1993, Scotts Mills, Oregon, earthquake, *Geophys. Res. Lett.* **22,** 13–16.

Pavlides, S. B., N. C. Zouros, A. A. Chatzipetros, D. S. Kostopoulos, and D. M. Mountrakis (1995). The 13 May 1995 western Macedonia, Greece (Kozani Grevena) earthquake; preliminary results, *Terra Nova* **7,** 544–549.

Patton, H. J. and G. Zandt (1991). Seismic moment tensors of western U.S. earthquakes and implications for the tectonic stress field, *J. Geophys. Res.* **96,** 18245–18259.

Ritsema, J. and T. Lay (1993). Rapid source mechanism determination of large (Mw ≥ 4.5) earthquakes in western United States, *Geophys. Res. Lett.* **20,** 1611–1614.

Romanowicz, B. A. (1982). Moment tensor inversion of long-period Rayleigh waves: a new approach, *J. Geophys. Res.* **87,** 5395–5407.

Romanowicz, B., D. Dreger, M. Pasyanos, and R. Urhammer (1993). Monitoring strain release in central and northern California using broadband data, *Geophys. Res. Lett.* **22,** 1643–1646.

Sipkin, S. A. (1982). Estimation of earthquake source parameters by the inversion of wave-form data: synthetic waveforms, *Phys. Earth Planet. Interiors* **30,** 242–259.

Taymaz, T., J. Jackson, and D. McKenzie (1991). Active tectonics of the north and central Aegean Sea, *Geophys. J. Int.* **106,** 433–490.

Thio, H.-K. and H. Kanamori (1995). Moment tensor inversions for local earthquakes using surface waves recorded at TERRAscope, *Bull. Seism. Soc. Am.* **85,** 1021–1038.

Trampert, J. and H. H. Woodhouse (1995). Global phase velocity maps of Love and Rayleigh waves between 40 and 150 seconds, *Geophys. J. Int.* **122,** 675–690.

Urhammer, R. (1992). Broadband near-field moment tensor inversions, *EOS* **73,** F375.

Department of Earth and Planetary Sciences
Harvard University
Cambridge, Massachusetts 02138

Manuscript received 10 July 1997.